Calibration, data processing, and maintenance of the United States Department of Agriculture high-resolution ultraviolet spectroradiometers

Peter Kiedron
State University of New York at Albany
Atmospheric Sciences Research Center
251 Fuller Road
Albany, New York 12203
and
NOAA/Earth System Research Laboratory
325 Broadway, MS: R/GMD-2
Boulder, Colorado 80305-3337
E-mail: peter.kiedron@noaa.gov

Mark Beauharnois
Jerry Berndt
State University of New York at Albany
Atmospheric Sciences Research Center
251 Fuller Road
Albany, New York 12203

Patrick Disterhoft
NOAA/Central UV Calibration Facility
325 Broadway, MS: R/GMD-2
Boulder, Colorado 80305

Lee Harrison
State University of New York at Albany
Atmospheric Sciences Research Center
251 Fuller Road
Albany, New York 12203

Joseph Michalsky
NOAA/Earth System Research Laboratory
325 Broadway, MS: R/GMD-2
Boulder, Colorado 80305

Gwen Scott
Colorado State University
Natural Resource Ecology Laboratory
Department 1499
Fort Collins, Colorado 80523-1499

Jim Schlemmer
State University of New York at Albany
Atmospheric Sciences Research Center
251 Fuller Road
Albany, New York 12203

James Slusser
Colorado State University
Natural Resource Ecology Laboratory
Department 1499
Fort Collins, Colorado 80523-1499

Abstract. The USDA ultraviolet radiation network currently includes four high-resolution spectroradiometers, located at Table Mountain, Colorado (deployed November 1998); the Atmospheric Radiation Measurement Climate Research Facility in Oklahoma (October 1999); Beltsville, Maryland (November 1999); and Fort Collins, Colorado (October 2002). These spectroradiometers contain Jobin Yvon's 1-m Czerny-Turner double additive spectrometers. The instruments measure total horizontal radiation in the 290- to 371-nm range, once every 30 min, with a nominal FWHM of 0.1 nm. We describe data quality control techniques as well as the data processing required to convert the raw data into calibrated irradiances. The radiometric calibration strategies using Central UV Calibration Facility FEL lamps that are directly NIST-traceable, portable field calibrators, and vicarious calibrations using data from UV multifilter rotating shadowband radiometers (MFRSRs) are discussed. Using direct-to-diffuse ratios from UV MFRSRs, we derive direct and diffuse high-resolution horizontal spectra from the collocated UV spectroradiometers of the USDA network. The direct-beam spectra can be used in a Langley regression that leads to spectroradiometric *in situ* calibration and to ozone column and aerosol optical depth retrievals. The high-resolution direct spectra are used to obtain the ozone column and aerosol optical depth in the 290- to 360-nm range at 0.1-nm resolution. A statistical summary of network performance is presented. [DOI: 10.1117/1.2769599]

Subject terms: atmospheric radiation; ultraviolet; spectral radiometry; spectroradiometer; ozone; aerosols; optical depth; calibration.

Paper 060369R received May 16, 2006; revised manuscript received Jan. 30, 2007; accepted for publication Feb. 7, 2007; published online Aug. 13, 2007. This paper is a revision of a paper presented at the SPIE conference on Ultraviolet Ground- and Space-based Measurements, Models, and Effects V, July, 2005, San Diego, Calif. The paper presented there appears (unrefereed) in SPIE Proceedings Vol. 5886.

1 Introduction

Four United States Department of Agriculture (USDA) UV spectroradiometers were deployed between November 1998 and October 2002. All four instruments perform measurements of total horizontal irradiance at the same operating frequency: one scan from 290 to 360 nm (or 371 nm after October 2004) in steps of $\Delta\lambda = 0.1$ nm once every 30 min during daylight hours with a nominal full width at half maximum (FWHM) of 0.1 nm. The spectroradiometer

0091-3286/2007/$25.00 © 2007 SPIE

Table 1 Statistics of instrument performance until June 14, 2004.

	U111 Table Mt., Colorado	U211 Billings, Oklahoma	U311 Beltsville, Maryland	U411 Fort Collins, Colorado
Field deployment date	11/23/98	10/28/99	11/25/99	10/22/02
Days in field until June 14, 2004	2056	1692	1653	600
Number of outage days	740	471	542	204
Number of operational days	1316	1221	1111	396
Operational days/days in field (%)	64.01	72.16	67.21	66.00
Number of outage periods	57	57	25	11
Average length of outage period (days)	12.98	8.26	21.68	18.54
25% of outages were no longer than (days)	1	1	2	1
50% of outages were no longer than (days)	2	3	5	6
75% of outages were no longer than (days)	7	6	16	17
Longest outage period (days)	217	109	162	130
Number of expected scans	31,025	29,001	26,047	9,180
Fraction of scans received on operational days (%)	93.14	95.70	98.60	97.02
Fraction of scans parsed on operational days (%)	92.72	95.27	98.53	96.96
Fraction of scans accepted on operational days (%)	91.31	91.87	94.06	93.59

specifications such as resolution, out-of-band rejection, and Poisson signal precision were verified during the 1997 intercomparison of ultraviolet spectroradiometers, where the prototype of the first instrument was presented.[1] The slit function, stray light, cosine response, wavelength equation, and details on the auxiliary measurements—consisting of dark scans and scans of the internal mercury lamps and two internal incandescent calibration lamps (called C1 and C2)–were discussed by Harrison et al.[2] U111, the instrument located at Table Mountain, Colorado, was operated during the 2003 intercomparison of ultraviolet spectroradiometers. The initial results on instrument calibration and operation history were presented by Beauharnois et al.[3]

In Sec. 2 we present a statistical summary of network performance and data quality control. Since initial deployment, the instruments have gone through a series of fixes and upgrades. We discovered and solved problems and have arrived at initial estimates of the mean time between failures (MTBF) for various parts and subsystems. We describe the upgrades and maintenance in Sec. 3.

We outline data reduction algorithms in Sec. 4 with an emphasis on wavelength calibration. In Sec. 5 several approaches to radiometric calibration are presented. In Sec. 6 we discuss data products. Finally, in Sec. 7, we demonstrate several applications of data in retrievals of ozone and aerosol optical depth.

2 Data Quality Control

In the normal mode of operation, each of the UV instruments performs the same repeating sequence of scans as follows: a dark scan with the fore optic shutter closed, followed by a solar scan at half-hour intervals from 290 to 360 nm (371 nm after October 2004) in steps of $\Delta\lambda = 0.1$ nm, followed by another dark scan, followed by a wavelength registration scan using the internal mercury lamp to measure the $\lambda = 296.728$-nm mercury line.

At night, one multiline mercury calibration scan is performed at wavelengths 289.359, 296.728, 312.566, 334.148, 365.0146, 404.6561, and 407.781 nm, and the internal incandescent calibration lamp C1 is burned and measured in the 280- to 408-nm range. Every 9 days, during the nighttime scan schedule, the internal incandescent calibration lamp C2 is burned and measured in the 280- to 408-nm range.

In the early morning hours, prior to the start of the daytime sequence of dark, solar, dark, and mercury scans, the data stream is closed and a new daily file is created. The previous day's raw file is then automatically transferred to the Atmospheric Sciences Research Center (ASRC) data server, where it is parsed and processed by a series of data-processing programs.

The summary of instrument performance is given in Table 1. Using U211 as an example, instrument perfor-

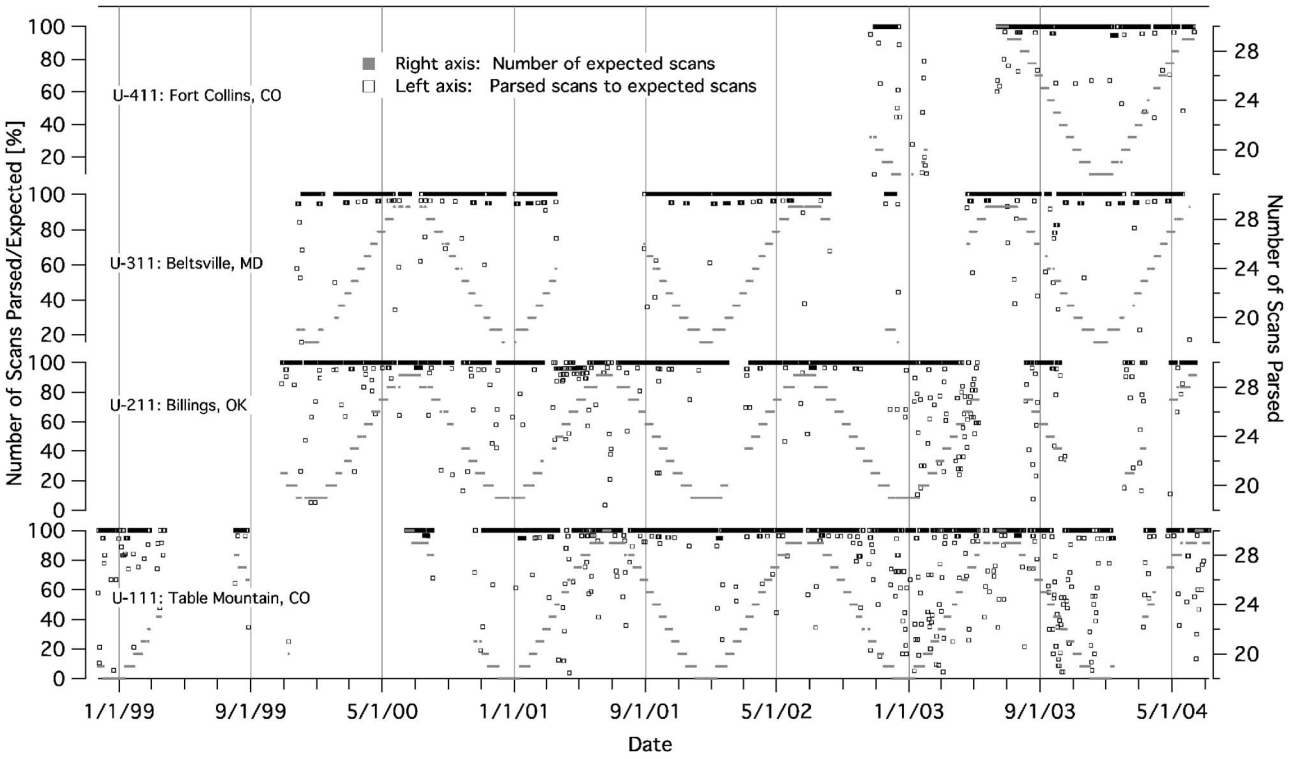

Fig. 1 Number of expected scans and percentage of processed scans for all four instruments.

mance can be summarized as follows. As of June 14, 2004, U211 has been in field operation for 1692 days, out of which it provided data for 1221 (72%). U211 sustained 57 data outages totaling 471 days. Of the outages, 25% were 1 day long, 50% were at most 3 days long, and 75% were at most 6 days long (see Fig. 1). The longest outage lasted for 109 days. During the 1221 operational days the instrument received 95.7% of the 29,001 expected solar scans. Subsequent to data parsing and quality control, 91.87% of the expected solar scans were accepted.

3 Maintenance

By June 2004, the four instruments had sustained a total of 150 separate data outage periods. Most outages were of short duration (less than 6 days) and typically resulted from power failures and computer and communication problems. The response time to address these failures was on average 2.5 days in Billings, OK, and Table Mountain, CO, and was somewhat longer at 5.5 days in Beltsville, MD, and Fort Collins, CO. Communication with both U311 and U411 is done via a modem ppp connection, which makes remote diagnosis more difficult.

The most serious breakdown occurred at Billings, OK, when the steel bearings of the U211 spectrometer drive rusted, and the replacement from Jobin Yvon in France took longer than expected and resulted in 109 days of down time. Subsequent to that rusting problem, the UV spectroradiometers in Maryland (U311) and Oklahoma (U211) were equipped with dehumidifiers.

The connection between the stepper motor and motor driver board developed a difficult-to-diagnose intermittent problem that resulted in occasional missing steps during scanning in some units. The problem was eventually diagnosed as electrical current arcing between the cable connector and stepper motor leads and was solved by using a soldered cable connection to the motor.

On two occasions (Billings and Table Mountain) birds pecked holes in the Teflon diffusers. The diffusers were replaced after we designed and installed the first model of a bird-deterring device. The device went through two more generations of improvements. In September 2001, the heavily soiled diffuser of U111 was replaced.

On average, we had to replace internal mercury lamps once a year. The most recent batch of these internal mercury lamps appear to have a shorter life, and their output is much less stable. Also, once a year we have to replace or refurbish the dry-air supply pump. The air conditioning (HVAC) unit maintenance is carried out by the manufacturer on an as-needed basis. Firmware upgrades have been made to all four UV instruments to facilitate the automatic operation of the portable field calibrators. With the exception of the field technician having to place the portable calibrator over the diffuser and plug in the calibrator, these calibrations are intervention-free. The normal scanning schedule was not changed as a result of the firmware upgrades.

After October 2004, we extended the upper limit of the scanning range from 360 to 371 nm, in order to capture the longest-wavelength (368 nm) channel of the UV Multifilter Rotating Shadowbanding Radiometer (MFRSR).

We also developed a Web-based system called CMATS (UV Calibration, Maintenance and Tracking System) to fa-

Table 2 Dark signal and coefficients *A* and *B* of wavelength equation.

	U111 Table Mt., Colorado	U211 Billings, Oklahoma	U311 Beltsville, Maryland	U411 Ft. Collins, Colorado
Field deployment date	11/23/98	10/28/99	11/25/99	10/22/02
Dark minimum (Hz)	0.00	0.12	0.00	0.10
Dark average (Hz)	0.29	0.22	0.13	0.15
Dark maximum (Hz)	1.29	0.93	1.14	0.28
Average wavelength equation A coefficient [nm/(200 steps)]	0.09996	0.10000	0.10001	0.10002
Maximal wavelength error (nm) at 360 nm due to $\pm\Delta A$ variation	0.0061	0.0081	0.0078	0.0029
Nominal wavelength equation coefficient *B* (nm)	290	290	290	290
1-σ variation of actual *B* coefficient (nm) from Hg centroids	0.0024	0.0034	0.0019	0.0016
1-σ variation of *B* (nm) from Fraunhofer algorithm	0.0068	0.0074	0.0069	0.0053
B(Fraunhofer) – *B*(centroids) (nm)	0.1154	0.1355	0.1152	0.1101

cilitate the logging of calibration, maintenance, and upgrade events and also to track instrument status and the location of the portable field calibrators.[3]

4 Data Reduction Algorithms

4.1 *Dark-Count Correction*

We compute a single daily dark count using all of the dark-count scans in a parsed daily UV data file, as no diurnal trend in dark counts is discernible within noise statistics. The dark count is subtracted from all solar scans contained in the same daily UV data file. Counts of each dark scan are normalized by the integration time (1 s). We then sort the normalized dark counts and compute the sum, average, minimum, and maximum values of the normalized counts. Then we apply a filter to remove outliers as a function of the average, minimum, and maximum. We then sort the final dark-count values, with outliers removed, and take the median as the final dark-count value to be used for that specific UV data file. In all four UV instruments, the dark counts are small and negligible for longer wavelengths (see Table 2). For U111 they exhibit seasonal variations (see Fig. 2), which are not present in the other three instruments.

4.2 *Wavelength Equation*

The solar spectrum is measured at grating positions $p = 0, \ldots, 700$, nominally every 0.1 nm (200 steps of the stepper motor). A slight, though detectable (±0.001 nm) nonlinearity in the steps-to-wavelength equation can be neglected. Thus a linear wavelength equation is used:

$$\lambda_p = Ap + B, \quad p = 0, \ldots, 700, \tag{1}$$

where $A = M \times \Delta\text{Step}$ for $\Delta\text{Step} = 200$. The wavelength equation coefficients *A* and *B* are obtained through two separate methods. The coefficient *M* is obtained from a linear fit between centroids in steps and wavelengths of the mercury lines at 289.359, 296.728, 312.566, 334.148, 365.015, 404.656, and 407.781 nm. The centroids are obtained from the once-a-day multiline mercury scan that is performed at night. The slope *M* is accepted if at least three good centroids are obtained. Then *A* is smoothed with an *RC* filter (see Fig. 2). In Table 2 the average values of *A* vary from 0.09996 to 0.10002 among the four instruments (all five digits are significant). The instantaneous values of *A* are very stable. The error in *A* has the largest effect at 360 nm ($p = 700$). If *A* were not measured at all, but rather the average value were used instead for the duration of deployment, the wavelength errors at 360 nm would still be less than ±0.0061 nm (see U111 in Table 2).

The wavelength coefficient *B* is obtained from processing the centroids of the 296.728-nm mercury line, which is scanned once for each solar scan. The centroid is estimated using the first-moment and dual-slope methods, and the resolution (FWHM) of this line is calculated.[2,3] The data are rejected if the centroids from the two methods differ by more than 0.0025 nm or if the FWHM departs from the nominal value by more than 0.004 nm. Then the remaining first moments are interpolated to generate the coefficient *B* for every solar scan in the daily file. In cases where all centroids are rejected, the centroid that violates the rejection criterion the least is used for the entire daily data.

In Fig. 3 we depict the maximal signal in counts when scanning the 296.728-nm line, and the fraction of accepted centroids. The dependence between signal strength and the number of good centroids can be discerned. Also, we observed that new mercury lamps in the beginning of their life cycle may have less stable intensity that results in centroids' skewness and their ultimate rejection. Furthermore,

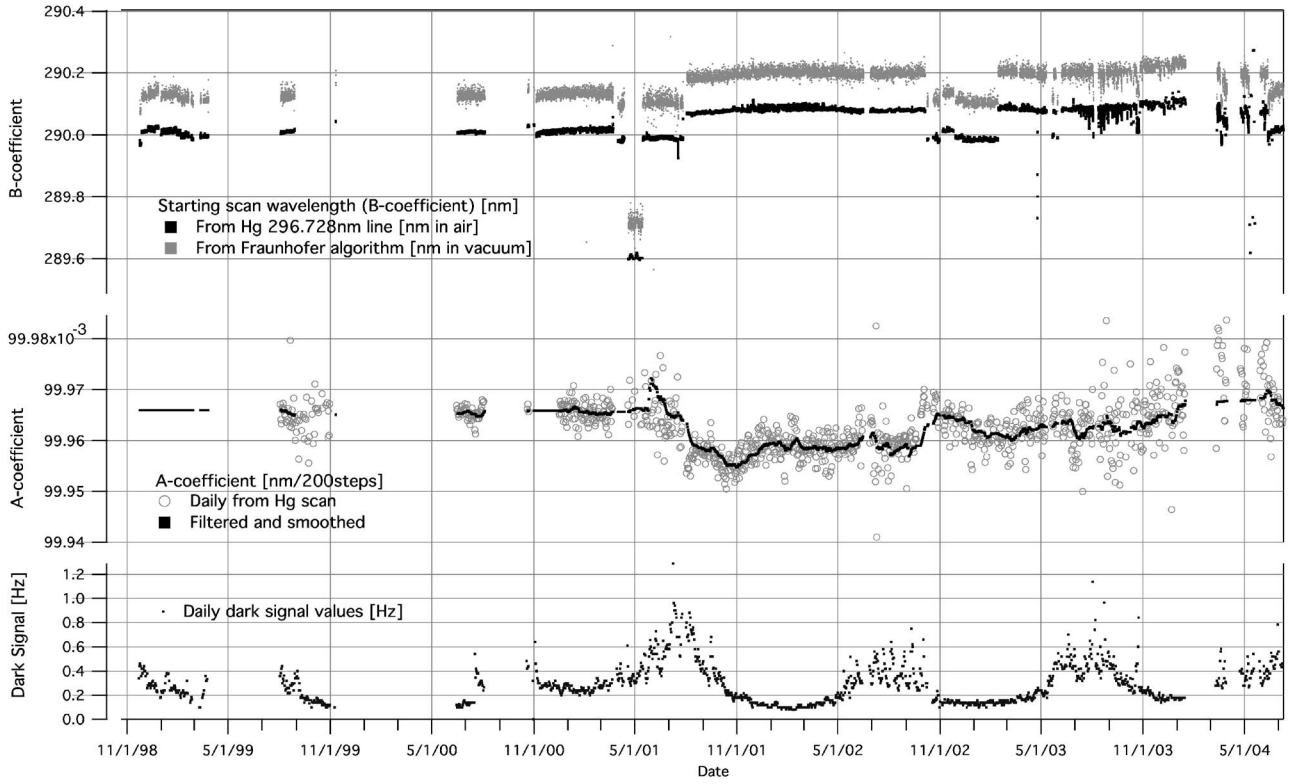

Fig. 2 Results for U111: instantaneous wavelength coefficient *B* from centroids and from Fraunhofer lines, daily wavelength coefficient *A*, and daily dark signal.

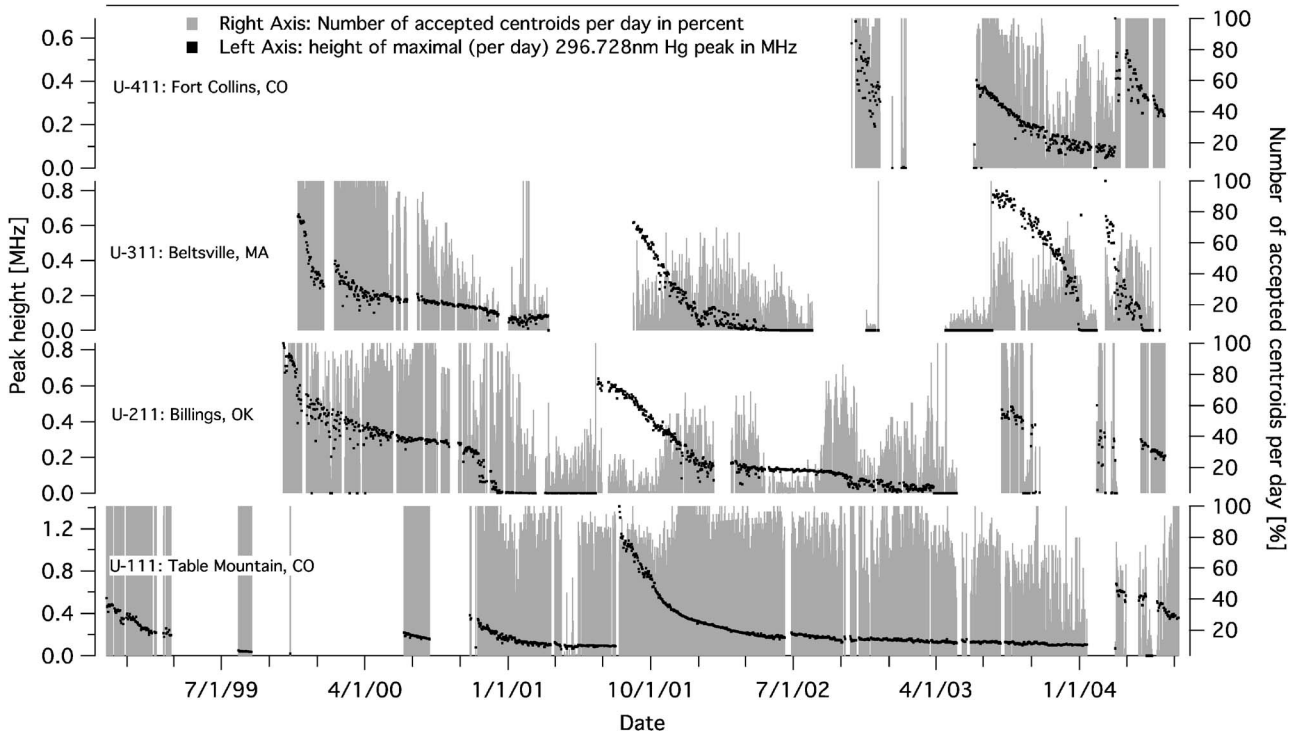

Fig. 3 Peak strength of 296.728-nm mercury line and percentage of good centroids per day for all four instruments.

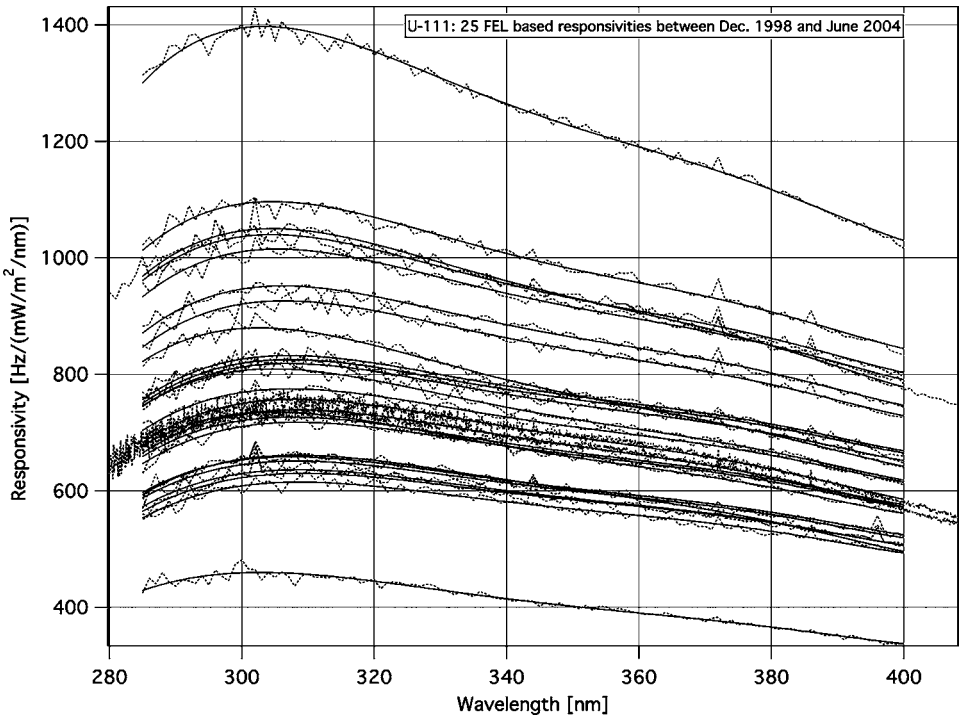

Fig. 4 Twenty-five responsivities of U111 obtained from measurements with CUCF horizontal FEL lamps between December 1998 and June 2004 (dotted lines) and fitted kernel responsivities (solid lines).

a second batch of mercury lamps (Fig. 3: U311 and U411 in 2003 and 2004) had a faster decay and may produce lower quality centroids than the lamps from the earlier batch.

4.3 *Wavelength Registration from Fraunhofer Lines*

The wavelength assignment of each solar scan is also derived from the Fraunhofer line spectrum measured in a vacuum. A correlation method between a reference spectrum with known wavelength-to-steps assignment and the measured spectrum was described by Beauharnois et al.[3] This method used wavelength assignment in vacuum of the extraterrestrial spectrum (ETS) that is based on the Solar Ultraviolet Spectral Irradiance Monitor (SUSIM) onboard the space shuttle during the ATLAS-2 and 3 missions.[4,5] The value of B from this method differs from the value derived from the centroid method, due to the air-vacuum wavelength difference. The Fraunhofer values are used when the mercury lamp does not produce usable centroids. The Fraunhofer method is also used to detect wavelength shifts during scanning. These occurred on a few occasions when the sine-drive mechanism failed (U211) or the stepper motor driver malfunctioned (all four units). The value of B from the centroid method (in air) and from the Fraunhofer method (in vacuum) are plotted in Fig. 2. The precision of the Fraunhofer method is approximately 0.007 nm (1σ), which is approximately 3 times worse than the centroid method (Table 2).

5 Radiometric Calibrations

5.1 *Responsivity from FEL Lamps*

Between 1998 and 2004, the responsivity of U111 was measured 25 times by the Central Ultraviolet Calibration Facility (CUCF). The CUCF calibrates U111 with its portable field calibrator, which was developed jointly with NIST.[6] The CUCF calibrator is designed to accommodate 1000-W FEL lamps that are operated with the long axis of the filament in the horizontal plane. The horizontally calibrated lamps are assigned a calibration certificate by direct comparison with NIST primary standards of spectral irradiance in the CUCF's Irradiance Scale Transfer System (ISTS). The development of the ISTS was another joint project between the CUCF and the Optical Technology Division of NIST. The system is capable of transferring the NIST spectral irradiance scale from the NIST primary standards of spectral irradiance to working standard lamps that operate in either the vertical or the horizontal orientation. Typically, the measurements were performed in the 285- to 400-nm range with a $\Delta=1$-nm sampling rate. The 25 responsivities are plotted in Fig. 4 (dotted lines). We analyze these results for the baseline distribution of the responsivity function that could be used to approximate any responsivity with a minimal number of parameters.

We normalize each responsivity $R_i(\lambda)$ by its integral $\|R_i(\lambda)\|$ $[r_i(\lambda)=R_i(\lambda)/\|R_i(\lambda)\|]$, and then we obtain the ensemble average $r(\lambda)=\langle r_i(\lambda)\rangle=\langle R_i(\lambda)/\|R_i(\lambda)\|\rangle$, where $\|\cdot\|$ denotes integration over wavelength and $\langle\cdot\rangle$ denotes ensemble average. We define the kernel responsivity $K(\lambda)$ as

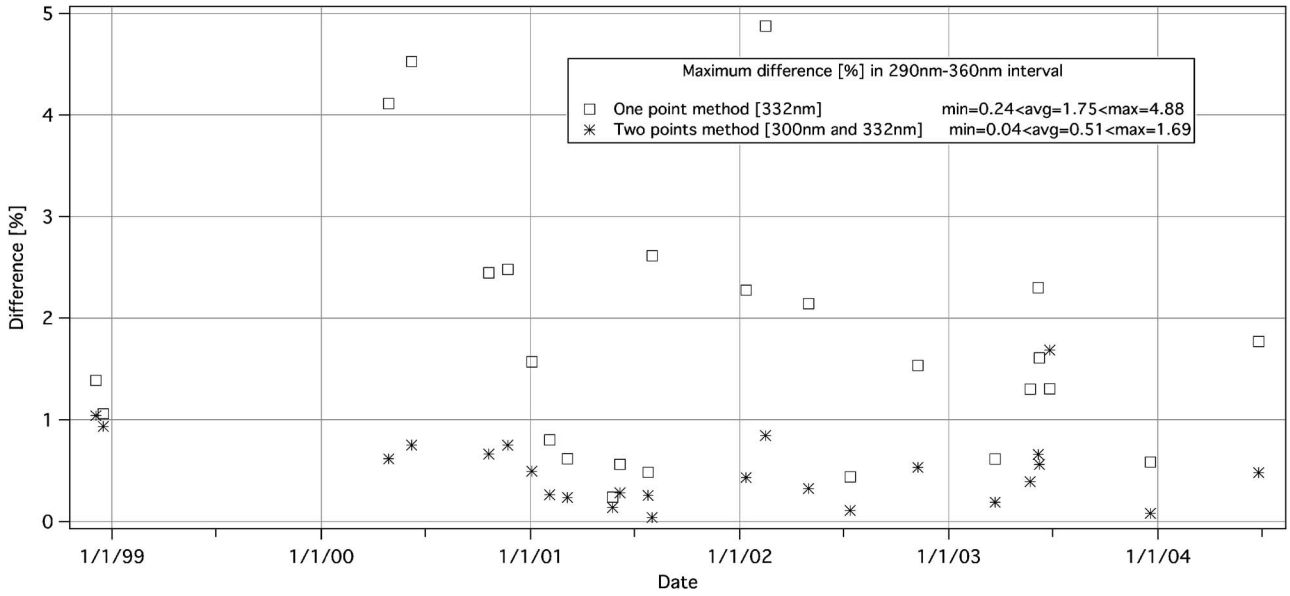

Fig. 5 Minimum, average, and maximum of calibration error in 290- to 360-nm range when using kernel responsivity scaled at 332 nm (squares) and with two-point scaling at 300 and 322 nm (crosses).

the sixth-degree polynomial fit to the ensemble average: $r(\lambda) \approx K(\lambda)$. Then we determined that the approximation

$$R_i(\lambda) \approx (a\lambda^2 + b\lambda + c)K(\lambda) \tag{2}$$

is better than 1.5% (rms) in all 25 cases. Therefore, $K(\lambda)$ greatly reduces the number of variables and can be used to approximate the responsivity of U111 at any time during its deployment. We stress here that during the time frame spanning the 25 measured responsivity cases, there were two diffuser changes, a fore-optics upgrade, and overall degradation of spectrometer throughput and photomultiplier tube (PMT) sensitivity.

In the narrower solar-scan spectral range of 290 to 360 nm, we tested whether even simpler approximations using two parameters $(b\lambda+c)K(\lambda)$ and one parameter $cK(\lambda)$ were feasible. In Fig. 5 the maximal errors for two such approximations are depicted. In the two-parameter case, the estimate is forced to be equal to the estimated responsivity at wavelengths 300 and 332 nm. Within the ensemble of 25 responsivity cases the maximal error is 0.5% on average, and greater than 1% in only two cases. In the one-parameter case, the estimate and the estimated responsivity are forced to be equal at 332 nm. On average, the error is 1.75%, and in three cases it is more than 3%.

5.2 *Portable Calibrators*

Four portable field calibrators were designed and built at ASRC for the purpose of easy and frequent calibration of the network of UV spectroradiometers. They are also used to calibrate visible-spectrum rotating shadowband spectroradiometers (RSSs)[7,8] in the 360- to 1100-nm spectral range, and the UV RSS[9] in the 295- to 385-nm spectral range.

A 250-W Gilway L7418 bulb is burned in a horizontal position. The housing has a concentric preheat chamber for channeling cool air to the bulb, so that the bulb always operates in 36°C air regardless of the outside air temperature. The air is introduced low in the chamber and removes the heat vertically away from the instrument's sensing surface. The bulb within the housing is positioned 27.9 cm above the instrument's diffuser surface. The lamp is controlled by a separate constant-current power supply of 10 A to an accuracy better than 0.005 A. The lamp's nominal current is 10.42 A, which is about 4% below its rating.

Each calibrator has an identification number assigned to it that is retired whenever a new bulb is installed or some modification, potentially altering the calibrator's irradiance, is implemented. The irradiance of a calibrator is derived through the transfer of irradiance from a CUCF FEL lamp via the U111 spectroradiometer at Table Mountain. Their mutual relative irradiances are checked using U369, a laboratory spectroradiometer identical to the field units, whenever two or more of the portable field calibrators are located at ASRC.

In Fig. 6 results of long-term stability testing for five portable calibrators, measured with the laboratory spectroradiometer U369, are presented. Note that calibrator P131 became calibrator P132 after a bulb change in August 2002. Data at wavelengths 300 and 368 nm are plotted using solid and dotted lines, respectively, and the remaining five wavelengths are plotted with individual dots.

Calibrator P128 was tested on 30 occasions between 2001 and 2004. The standard deviation of all 30 measurements was less than 2.5% at 368 nm and less than 1% at 300 nm, with $(\max-\min)/2$ being respectively 3.9% and 2.1%. The remaining wavelengths fall within these ranges. P130 was also tested 30 times; the standard deviation at 368 nm was lower (1.4%), and $(\max-\min)/2=2.1\%$. To appreciate the goodness of these results we emphasize that between these tests on the lab unit, the portable calibrators

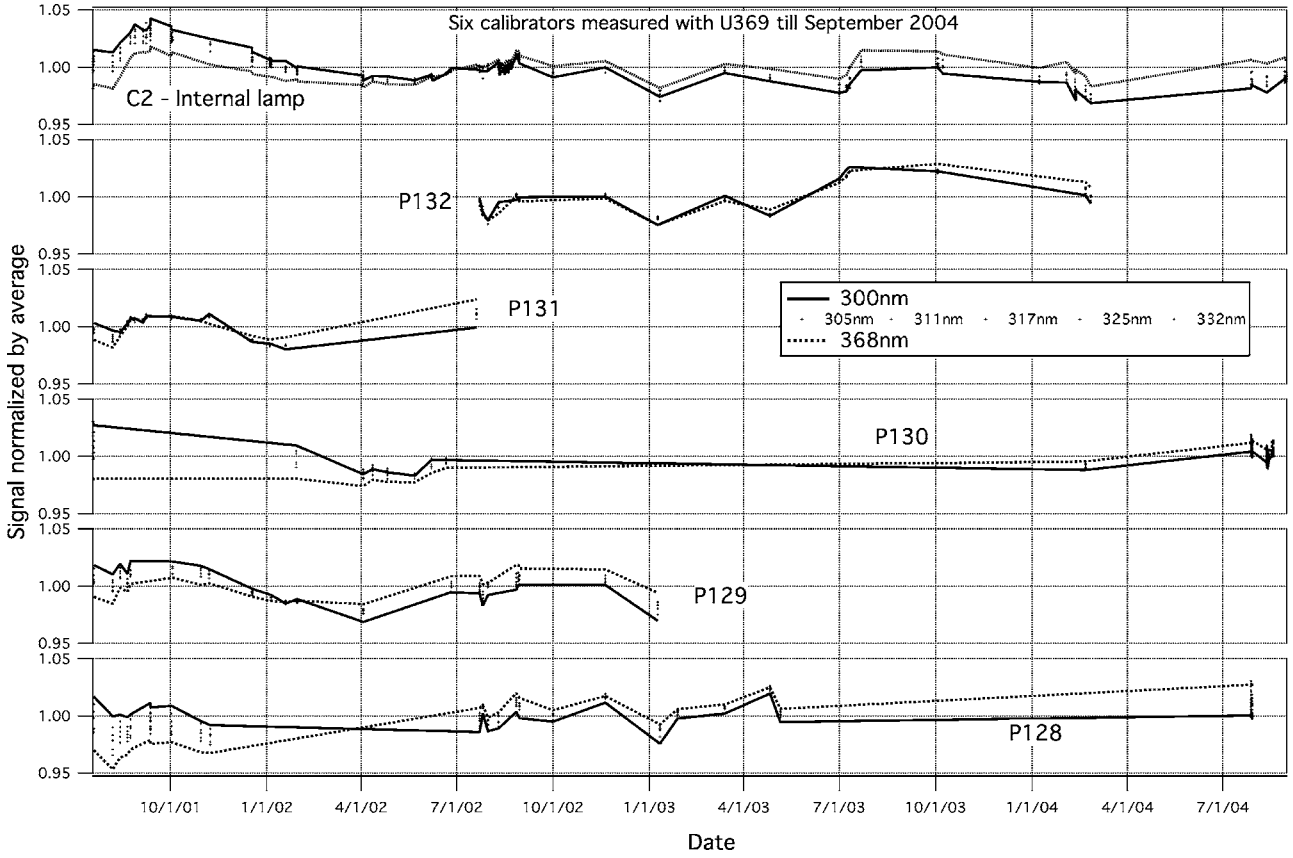

Fig. 6 Stability trends of portable calibrators as measured on laboratory spectroradiometer U369 at ASRC for seven wavelengths from 300 nm (solid lines) to 368 nm (dotted lines). Also, signals of the internal lamp are shown. Data are not corrected for U369 responsivity drift.

were shipped between all four field sites. Therefore, the impact of shipping on the irradiance scale of the portable calibrators, if any, was negligible.

The topmost traces in Fig. 6 are from measurements made with U369 using one of the internal incandescent lamps. When the output of the internal lamp is used to normalize signals generated by portable calibrators, the spectral dependence in the drift of the portable calibrators is eliminated.

Since May 2003, P128 has been used to calibrate the visible spectrum RSS deployed at the atmospheric radiation measurement site in Billings, Oklahoma. The RSS requires calibration in its 360- to 1060-nm spectral range. The portable calibrator was compared with the Li-Cor[10] calibrator, which in the 1999 study[11] showed exceptionally good agreement with the NIST FEL lamp irradiance standards. In Fig. 7, 15 semisimultaneous P128 and Li-Cor calibrations taken between May 2003 and October 2005 are compared. The standard deviation of ratios that include drifts and instability of both calibrators is approximately 1%.

5.3 *Vicarious Calibration*

Currently, each USDA UV spectroradiometer is collocated with a UV MFRSR. The UV MFRSR provides direct-beam, diffuse, and total horizontal irradiances at seven wavelength channels: 300, 305, 311, 317, 325, 332, and 368 nm.[12] In Sec. 5.1 we demonstrated that by using a kernel responsivity we can determine the responsivity for all wavelengths to within 1.75% if the responsivity is known at just one wavelength.

The UV MFRSR instruments are calibrated with the CUCF FEL lamps before and after each deployment. The total horizontal irradiance from the UV-MFRSR is used to obtain the responsivity of the UV spectroradiometers at the UV-MFRSR channel wavelengths. The responsivity at a given channel is the ratio of spectroradiometer counts at that channel to the irradiance according to the UV MFRSR. A more detailed mathematical description of this calibration process is given by Beauharnois et al.[3]

In Fig. 8 the responsivity at 332 nm obtained with the vicarious calibration method and the responsivity from FEL lamps are compared. Differences of ±10% are observed. Similar differences are obtained for 300 and 311 nm. Significantly larger differences result for the 305-, 317-, and 325-nm channels. We attribute these discrepancies to drift and calibration errors in the UV MFRSRs. When UV-MFRSR irradiances are corrected with V_0's from Langley regression plots, the 305-, 317-, and 325-nm channels become congruent with the other channels.

We are uncertain if all changes and shapes in the curve seen in Fig. 8 accurately reflect responsivity changes of U111. However, some variations can be identified and are

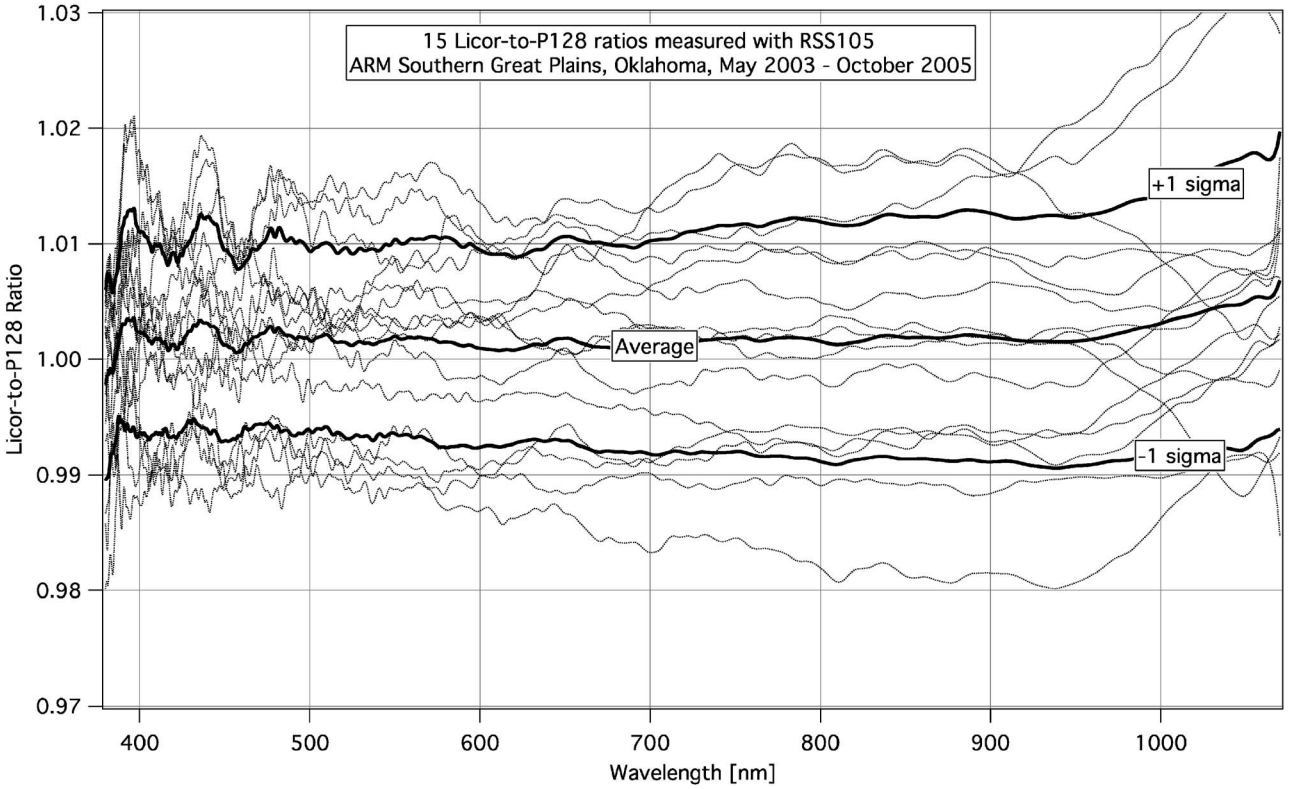

Fig. 7 Mutual stability between portable calibrator P128 and Li-Cor calibrator in 370- to 1060-nm range measured with the rotating shadowband spectroradiometer RSS105 at ARM Southern Great Plains Site in Oklahoma between May 2003 and October 2005.

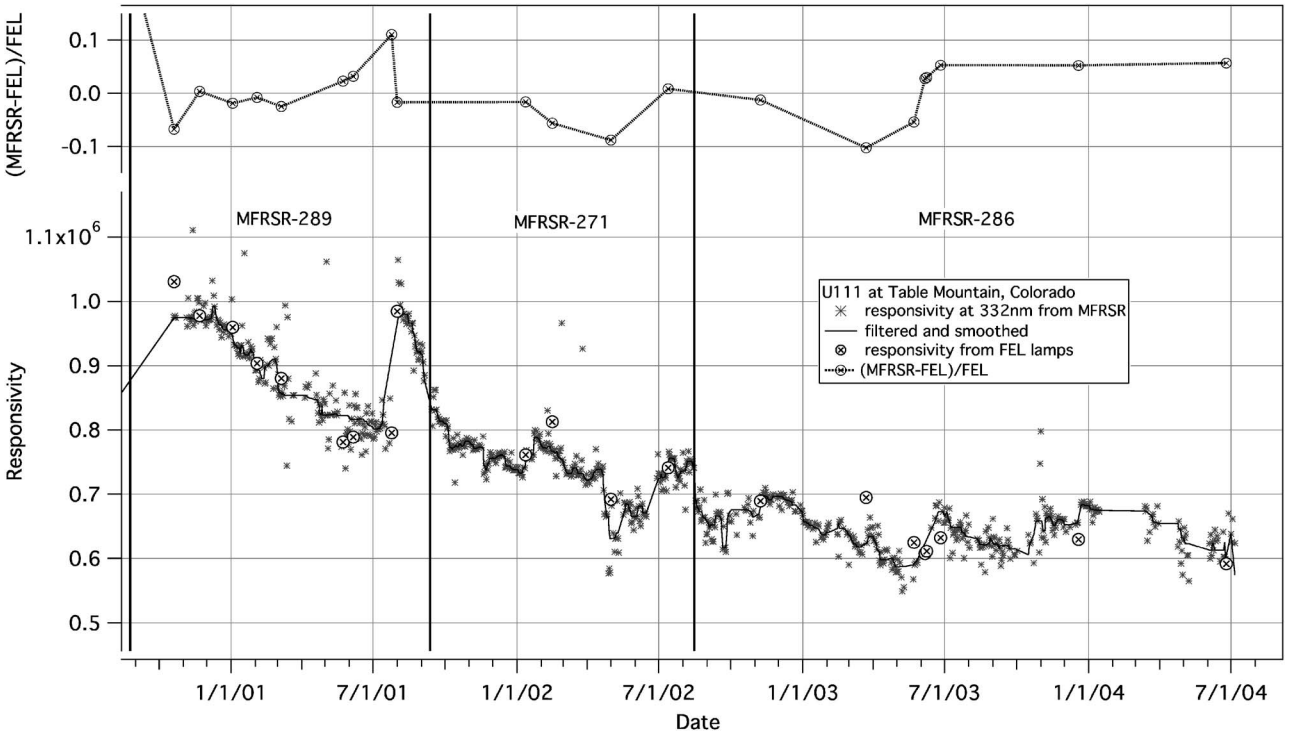

Fig. 8 U111's responsivity at 332 nm from CUCF FEL calibrations and from vicarious calibration based on 332-nm channel.

Table 3 Available classes of UV spectroradiometer calibration methods.

Calibration class	Subclass	Description
V	S	Vicarious calibration using single UV MFRSR channel
	M	Vicarious calibration using multiple UV-MFRSR channels
P		Portable field calibrator
F		FEL lamp calibration
H		Hybrid calibration

real. For instance, the sudden surge of responsivity in August 2001 and its subsequent decay are a result of the installation of a new diffuser.

6 Data Products

6.1 *Uncalibrated Solar Files*

We provide UV solar data, uncalibrated but normalized to 1-s exposure and dark-count-corrected, as files with filename extensions Q00.S.[13] For these Q00 files no responsivity was applied to the solar scan data. In addition to the actual solar scan data, these files contain coefficients for the linear time equation for each scan, so the time at every measured wavelength, in every solar scan, can be calculated. Also, the wavelength-equation coefficients A and B (both from the centroids and from the Fraunhofer method) and the dark-count removal value are included in the Q00 solar files. In each of the Q00 solar files we include statistics on centroid quality, mercury lamp strength, and multiline scan linear regression results including FWHM. Most of the data presented in Figs. 1 through 3 and Tables 1 and 2 were extracted from Q00 solar files.

6.2 *Calibrated Solar Files*

We have several classes of methods for generating calibrated solar files for all four USDA UV instruments. Table 3 provides a list of all of the available calibration methods and their descriptions. Currently, we generate two classes of calibrated solar data: vicarious calibrations based on the 332-nm channel from the UV-MFRSR data, and lamp-calibrated data from calibrations done using FEL irradiance lamps. The vicariously calibrated data are provided as files with QVS01.S filename extensions, and the FEL calibrated data with QF001.S filename extensions.[13] Lamp calibrations for the solar data are typically done manually, after the lamp calibration files have been processed offline. The vicarious calibration process is automatically run every day, as long as there is an appropriate collocated, calibrated UV-MFRSR file for the same date as the UV spectroradiometer data file.

6.3 *Direct-to-Diffuse Ratios*

A true direct-to-diffuse ratio $R=I_{\mathrm{dir}}/I_{\mathrm{dif}}$ is available, at a high sampling rate, from UV MFRSRs at seven wavelengths. In the 300- to 368-nm range it is reasonable to assume that R is linear between each two adjacent channel wavelengths. By synchronizing the linear interpolation with the wavelength position of the spectroradiometer we calculate the direct-to-diffuse ratio for all wavelengths in the 295- to 371-nm range. Below 300 nm we extrapolate from the 300- and 305-nm channels, and above 368 nm we extrapolate from the 332- and 368-nm channels. However, it should be noted that a linear extrapolation below 300 nm is not very reliable. From the total irradiance I_S that is uncor-

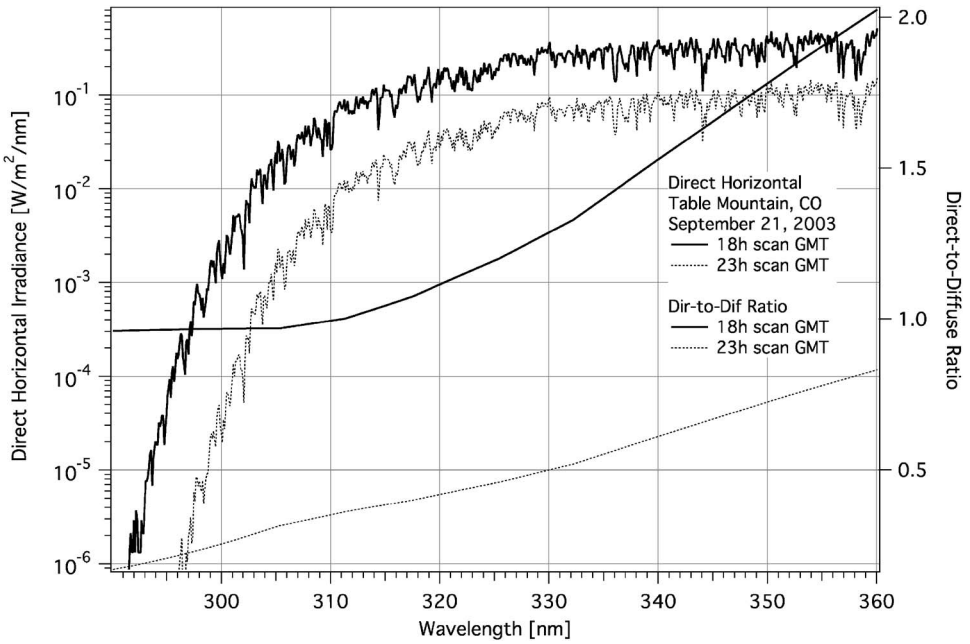

Fig. 9 Direct horizontal irradiance derived from U111 total irradiance and the direct-to-diffuse ratios from the collocated UV MFRSR.

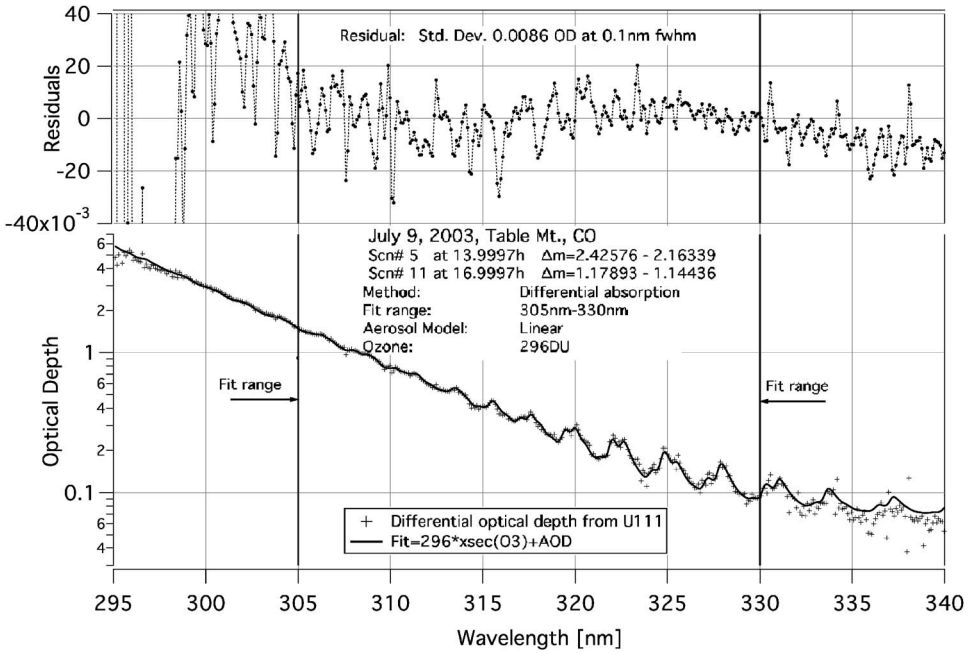

Fig. 10 Example of ozone retrieval with differential absorption method. Measured and fitted ozone and aerosol optical depths and the residuals from the rms fit are shown.

rected for cosine response, the direct horizontal and diffuse horizontal components are obtained as follows:

$$I_{\mathrm{dir}} = \frac{I_S R}{RC_{\mathrm{dir}} + C_{\mathrm{dif}}} \quad \text{and} \quad I_{\mathrm{dif}} = \frac{I_S}{RC_{\mathrm{dir}} + C_{\mathrm{dif}}}, \tag{3}$$

where C_{dif} and C_{dir} are the diffuse and direct cosine corrections, respectively, derived from the Ux11 angular response. Then the direct normal irradiance is given by

$$I = I_{\mathrm{dir}}/\cos(\mathrm{SZA}). \tag{4}$$

Using this approach, we obtain the high-resolution direct irradiance spectrum, and thus one can take advantage of the Beer-Lambert law in retrieval methods. For example, the retrievals of the ozone column and aerosol optical depth can be greatly simplified. The direct-to-diffuse ratios are saved as files with a filename extension Q00.R.[13] Then, from the Q00.R and Q00.S files, one can easily obtain high-resolution direct and diffuse horizontal irradiance scans using the equations (3) (see Fig. 9).

7 Application Examples

7.1 *Ozone Retrievals*

Ozone retrievals are based on the difference between optical depths for at least two wavelengths. In instruments such as Ux11, where measurements are performed sequentially in wavelength, the success of the retrieval is dependent on the stability of the atmosphere during, and between, the measurements of the specific wavelength. Otherwise, aerosol change or cloud passage may make ozone retrieval unreliable. The UV spectroradiometers scan at an approximate rate of 0.1 nm/(1.4 s). Thus, the atmospheric stability must be on the order of 7 min, as that is the time required to scan the 305- to 335-nm interval.

The retrieval method must be robust enough to identify suitable scans or scan intervals within a single scan. An additional complication in retrievals is that only a total irradiance is available. Thus aerosols, cloud coverage, and even surface albedo may affect ozone retrievals, as the effective air mass can be only estimated approximately. Despite these difficulties, retrievals from sequentially scanned total irradiance instruments are performed routinely.[14–17] As described in Sec. 6.3, a high-resolution direct irradiance can be derived with the auxiliary measurements from the collocated UV MFRSR. This direct component of total irradiance and the availability of the exact estimate of air mass in a direct beam makes retrievals much more accurate.[18]

7.1.1 *Differential absorption method*

The method of differential absorption is superior in its sensitivity level, as it is able to cancel instrument calibration errors and remove the high-frequency Fraunhofer structure at exactly the required resolution. However, its sensitivity is slightly reduced as noise from the two spectra that are ratioed is added. The disadvantage of this approach is that the differential optical depth is useful for retrievals only when the measured parameters such as the ozone column or aerosol optical depth is the same for the two ratioed spectra. This method is demonstrated on one case that is presented in Fig. 10.

We calculate the differential optical depth from two spectra I_i and I_j as follows:

$$\tau = \frac{\ln(I_i/R_i) - \ln(I_j/R_j)}{m_j - m_i}, \tag{5}$$

where R_i and R_j are calculated Rayleigh scattering transmittances and m_i and m_j are ozone air masses. All I, R, and

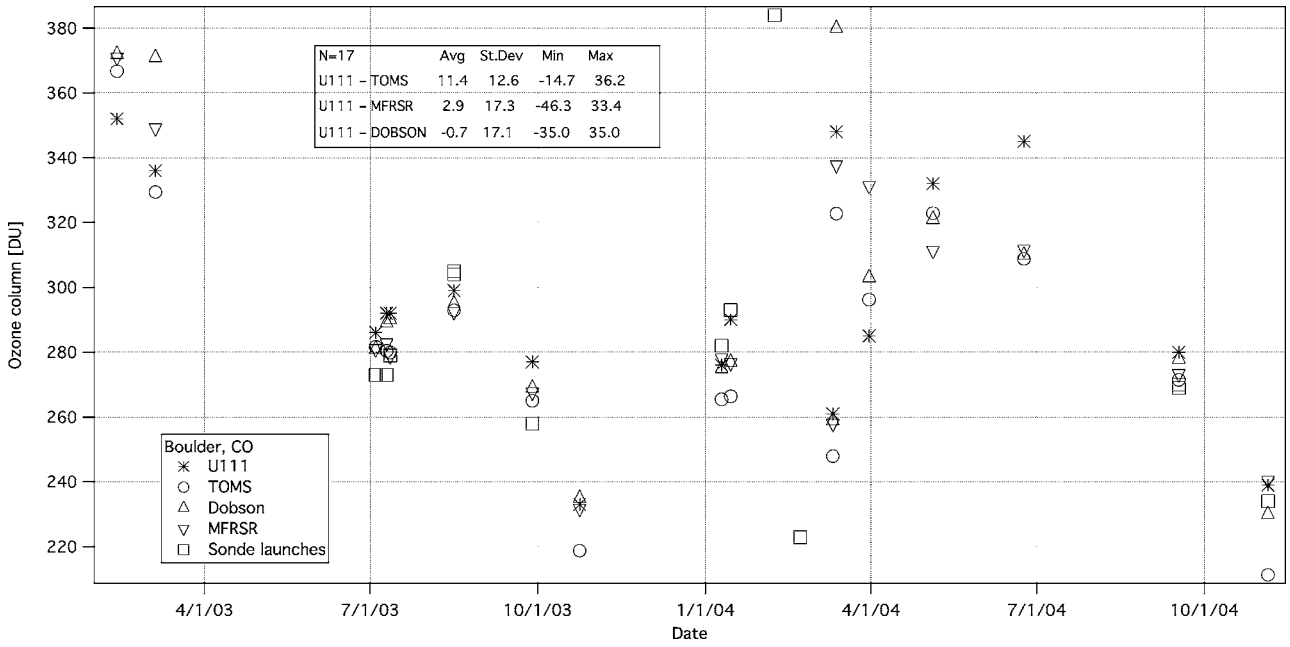

Fig. 11 Comparison of ozone from U111 with differential absorption method and ozone columns according to TOMS, MFRSR, and Dobson for 17 clear-sky cases. Also, results from ozone sonde launches are shown.

m are functions of time, and time is a function of wavelength in the scanning instrument. The ozone column and aerosols are obtained using a least-squares fit:

$$\min_{DU,\alpha,\beta} \int |\tau(\lambda) - DU \cdot a(\lambda) - A(\lambda,\alpha,\beta)|^2 \delta\lambda \tag{6}$$

with respect to three parameters DU, α, β, where DU is the ozone column in Dobson units, a(λ) is the ozone absorption cross section, and $A(\lambda,\alpha,\beta)$ is a two-parameter aerosol model:

$$A(\lambda,\alpha,\beta) = \beta + \alpha\lambda \quad \text{or} \quad A(\lambda,\alpha,\beta) = \beta\lambda^{-\alpha}. \tag{7}$$

Smoothing of the optical depth in wavelength space improves the stability of the method. Subsequently, retrievals were performed by averaging 5 to 10 adjacent wavelengths. The fit was performed in the 305- to 330-nm integration interval, although we did observe that results were slightly sensitive to the selection of that wavelength integration interval.

On a given day n spectra are available, leading to $n(n-1)/2$ combinations. We calculate the average standard deviation of Poisson noise (based on PMT counts) in the integration interval for all possible (i,j) combinations. Then we select 20 combinations with the highest signal-to-noise ratio. This implies that scan pairs with large differences in air masses are selected. Then, using the 20 pairs of scan combinations, we calculate the average from among those with the smallest fit residuals. The derived ozone column is in some sense a weighted average: $\mathrm{DU}_{ij}=(\mathrm{DU}_i m_i - \mathrm{DU}_j m_j)/(m_i - m_j)$. This average is equal to the actual ozone column when the column is the same for both i and j. However, when the ozone column is not constant, even the average of all available DU_{ij} is not exactly equal to the average ozone. But it is possible to estimate the diurnal ozone trend from all DU_{ij} by finding optimal parameters a and b in the time trend $\mathrm{DU}=at+b$ equation that minimize differences:

$$\mathrm{DU}_{ij} - \frac{(at_i + b)m_i - (at_j + b)m_j}{m_i - m_j}. \tag{8}$$

Retrievals were performed for 17 clear days in 2003 and 2004 and compared with retrievals from the collocated UV MFRSR and from TOMS and Dobson measurements in Boulder, Colorado. In Fig. 11, ozone columns from the four instruments are plotted together, including several sonde readings provided by the Climate Modeling and Diagnostics Laboratory (CMDL). The differences between U111 and the other three instruments are comparable. The standard deviation of those differences varies from 12 to 17 DU for different instrument pairs.

The differential absorption method is less suitable for the retrieval of aerosol optical depth, as the aerosols may change at a faster rate and by larger magnitudes than ozone column trends.

7.1.2 *Direct spectrum synthesis method*

To obtain ozone or aerosols at a given instant, a direct synthesis of spectra, at least in the vicinity of ozone absorption features, is necessary. In this method, we calculate the optical depth as follows:

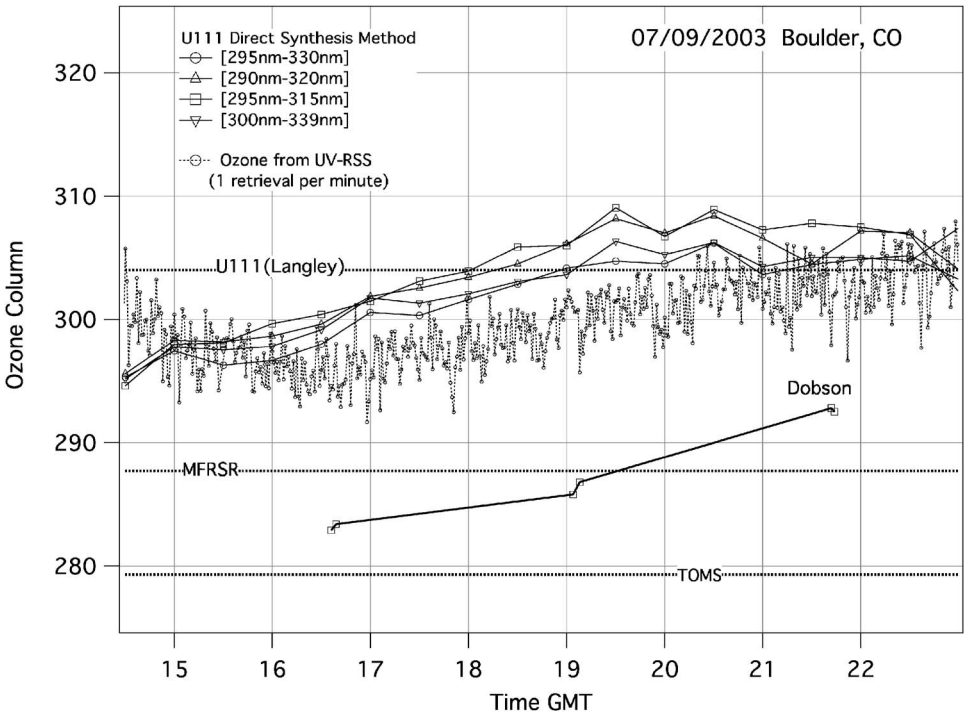

Fig. 12 Retrieval of ozone for 18 consecutive scans, using four different rms-fit spectral intervals, is compared with results from Dobson, MFRSR, TOMS, UV RSS, and ozone from the optical depth obtained from Langley regression on U111 data.

$$\tau(\lambda) = -\frac{1}{m}\ln\left(\frac{I(\lambda)}{\int s(\lambda',\lambda)\cdot \mathrm{I}_o(\lambda')\cdot\exp[-\tau_P(\lambda')m_R]d\lambda'}\right) \tag{9}$$

where the high-resolution extraterrestrial solar irradiance I_0 is multiplied by the Rayleigh scattering transmittance and smoothed $s(\lambda',\lambda)$ with a triangular slit function that for U111 has the dependence $\mathrm{FWHM}(\lambda)=0.1(1.7779-0.0022901\lambda)$. We used Bernhard et al.'s[19] ETS at $\Delta\lambda=0.05$ nm. This ETS spectrum was obtained using the Kitt Peak solar flux atlas,[20] scaled to maximize agreement with Gueymard's low-resolution ETS.[21] This ETS provided lower residuals than the one previously used by us in Ref. 18, where we scaled Kurucz's[22] high-resolution (1-cm^{-1}) ETS with a low-resolution SUSIM ETS. To further reduce residuals we smoothed the optical depth (1 nm=10 steps) prior to performing the least-squares fit in the Eq. (6). This method produces higher residuals than the differential absorption method. Nevertheless, it is adequate for ozone retrieval, particularly when it is based on a fit in the shorter-wavelength region, where ozone cross sections exhibit rapid growth that cannot be matched by any reasonable aerosol extinctions. Then, the fit is not dependent on matching of small optical absorption artifacts, in contrast with the methods used in retrieval from Dobson or UV-MFRSR instruments. We expect a lower sensitivity to ozone profiles, as the ozone cross sections are less sensitive to temperature at shorter wavelengths. Unlike the differential absorption method, using this method one can obtain estimates of diurnal ozone trends directly.

In Fig. 12, the retrievals from all available scans for July 9, 2003 are presented. Retrievals were performed using several integration intervals. The part of the trend shown by six Dobson measurements was captured by this retrieval method. Also the results from once-a-minute retrievals from the UV RSS[23] are included.

7.2 *Langley Regression*

The direct normal irradiance from Eq. (4) can be used in Langley plots.[24] In the current mode of operation, U111 measures one spectrum from 290 to 371 nm once every 30 min. Thus, any particular wavelength is measured in only 10 to 15 separate air masses between winter and summer. The Langley regression plot can only be successful during exceptionally clear and stable atmospheric conditions when only a few points are lost to outliers. Since each wavelength is measured at different times, there is limited coherence between Langley regression parameters at different wavelengths. Nevertheless, we found days when the Langley regression produced good optical depth and V_0, such as is shown for the Langley results for July 9, 2003 in Fig. 13. We compared the V_0 spectrum with Bernhard's ETS spectrum. The V_0 from this single Langley plot (of 12 points only) is on average 11% lower than the ETS in the 299- to 360-nm range. The standard deviation of the ratio V_0/ETS is only 0.027, indicating a very good reproducibility of Fraunhofer structure by this single Langley regression. A small wavelength adjustment (0.012-nm shift towards longer wavelengths) was required to minimize the difference between V_0 and ETS high-frequency features. The optical depth τ contains clearly visible ozone absorption features. The optical depth τ from Fig. 13 was used to

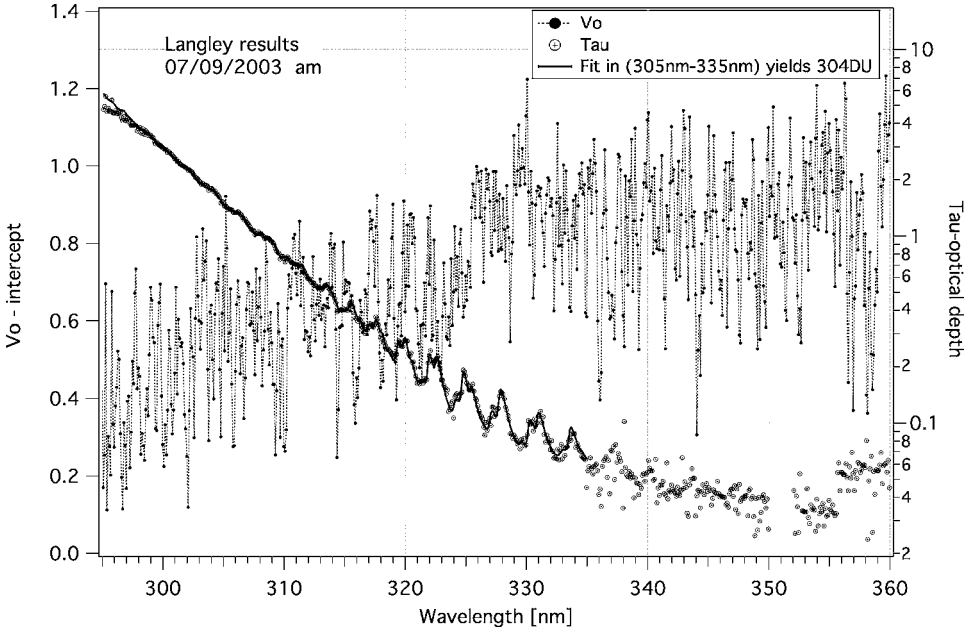

Fig. 13 Intercept V_0 and optical depth τ obtained from a Langley regression using derived direct normal irradiance from all morning scans on July 9, 2003.

retrieve ozone (without smoothing in the 305- to 335-nm range). The value of ozone compares well with those from other methods and instruments (see Fig. 12).

8 Summary

We have described the operation, maintenance, and calibration of four USDA 1.0-m reference double spectrometers. Two of them—U111 at Table Mountain and U411 in Fort Collins, Colorado—remain in regular operation. The other two fielded spectrometers are not in regular operation due to manpower constraints. These instruments have exceptional Lambertian angular response,[2] wavelength accuracy, and precision. The radiometric stability is well characterized by daily internal lamp stability checks and less frequent absolute calibrations made with a 1000-W NIST-traceable standard-lamp portable calibrator[6] and with ASRC portable calibrators. The data can be made more useful by partitioning the measured total horizontal spectral irradiance into direct and diffuse, using data from a collocated UV MFRSR. Since the UV MFRSR uses the same filter, detector, and amplification, the diffuse-to-direct ratio is accurate to ±1%.[25] It now becomes possible to retrieve the total ozone column and aerosol optical depth using the spectrometer pseudodirect beam, which can even be Langley-calibrated. These retrievals compare well with those from the collocated UV MFRSR.

Acknowledgments

We thank the anonymous reviewers for an exceptionally thorough and constructive critique that was invaluable in making this paper better. We acknowledge USDA funding via contract CSREES 2005-06283.

References

1. K. Lantz, P. Disterhoft, E. Early, A. Thompson, J. DeLuisi, P. Kiedron, L. Harrison, J. Berndt, W. Mou, T. J. Ehramjian, L. Cabausua, J. Robertson, D. Hayes, J. Slusser, D. Bigelow, G. Janson, A. Beaubian, and M. Beaubian, "The 1997 North American interagency intercomparison of ultraviolet monitoring spectroradiometers," *J. Res. Natl. Inst. Stand. Technol.* **107**, 19–62 (2002).
2. L. Harrison, J. Berndt, P. Kiedron, and P. Disterhoft, "United States Department of Agriculture reference ultraviolet spectroradiometer: current performance and operational experience at Table Mountain, Colorado," *Opt. Eng.* **41**(12), 3096–3103 (2002).
3. M. Beauharnois, P. Kiedron, and L. Harrison, "The USDA high-resolution UV radiation network: maintenance, calibration and data tools," *Proc. SPIE* **5545**, 90–101 (2004).
4. J. A. Kaye and T. L. Miller, "The ATLAS series of shuttle missions," *Geophys. Res. Lett.* **23**(17), 2285–2288 (1996).
5. M. E. vanHoosier, "Solar ultraviolet spectral irradiance data with increased wavelength and irradiance accuracy," in *Ultraviolet Atmospheric and Space Remote Sensing: Methods and Instrumentation*, R. E. Huffman and C. G. Stergis, Eds., *Proc. SPIE* **2831**, 57–64 (1996).
6. E. A. Early, E. A. Thompson, and P. Disterhoft, "Field calibration unit for ultraviolet spectroradiometers," *Appl. Opt.* **37**(28), 6664–6670 (1998).
7. L. Harrison, M. Beauharnois, J. Berndt, P. Kiedron, J. Michalsky, and Q. Min, "The rotating shadowband spectroradiometer (RSS) at SGP," *Geophys. Res. Lett.* **26**, 1715–1718 (1999).
8. P. W. Kiedron, L. Harrison, J. J. Michalsky, Jr., J. Schlemmer, and J. L. Berndt, "Data and signal processing of rotating shadowband spectroradiometer (RSS) data," *Proc. SPIE* **4815**, 58–72 (2002).
9. P. W. Kiedron, L. H. Harrison, J. L. Berndt, J. J. Michalsky, and A. F. Beaubien, "Specifications and performance of UV rotating shadowband spectroradiometer (UV-RSS)," *Proc. SPIE* **4482**, 249–259 (2001).
10. Li-Cor, Inc., *1800-02 Optical Radiation Calibrator Instruction Manual*, P.O. Box 4425, Lincoln, NE 68504 (1990).
11. P. W. Kiedron, J. J. Michalsky, J. L. Berndt, and L. C. Harrison, "Comparison of spectral irradiance standards used to calibrate shortwave radiometers and spectroradiometers," *Appl. Opt.* **38**, 2432–2439 (1999).
12. W. Gao, J. Slusser, J. Gobson, G. Scott, D. Bigelow, J. Kerr, and B. McArthur, "Direct-sun column ozone retrieval by the ultraviolet multifilter rotating shadow-band radiometer and comparison with those from Brewer and Dobson spectrophotometers," *Appl. Opt.* **40**, 3149–3155 (2001).
13. ftp://oink.asrc.cestm.albany.edu/pub/U*X*11/calibrated/, where $X=1,2,3,4$.
14. K. Stamnes, J. Slusser, and M. Bowen, "Derivation of total ozone abundance and cloud effects from spectral irradiance measurements," *Appl. Opt.* **30**(30), 4418–4426 (1991).
15. D. Masserot, J. Lenoble, C. Brogniez, M. Houet, N. Krotkov, and R. McPeters, "Retrieval of ozone column from global irradiance measurements and comparison with TOMS data: a year of data in the

Alps," *Geophys. Res. Lett.* **29**(9), 23 (2002).
16. G. Bernhard, C. R. Booth, and R. D. McPeters, "Calculation of total column ozone from global UV spectra at high latitudes," *J. Geophys. Res.* **108**(D17), 4532, (2003).
17. G. Bernhard, R. D. Evans, G. J. Labow, and S. J. Oltmans, "Bias in Dobson total ozone measurements at high latitudes due to approximations in calculations of ozone absorption coefficients and airmass," *J. Geophys. Res.* **110**, D10305, (2005).
18. P. Kiedron, M. Beauharnois, and L. Harrison, "Derived direct irradiance from high resolution UV spectroradiometer uses: Langley regression radiometric calibration ozone column and aerosol retrievals," *Proc. SPIE* **5886**, 32–40, 588605 (2005).
19. G. Bernhard, C. R. Booth, and J. C. Ehramjian, "Supplement to Version 2 data of the National Science Foundation's Ultraviolet Radiation Monitoring Network: South Pole," *J. Geophys. Res.* **109**, D21207, (2004).
20. R. L. Kurucz, I. Furenlid, J. Brault, and L. Testerman, *Solar Flux Atlas from 296 to 1300 nm*, *National Solar Observatory Atlas No. 1, Harvard Univ. Press*, Cambridge, MA ftp://ftp.noao.edu/fts/fluxatl/ (1984).
21. C. Gueymard, "The Sun's total and spectral irradiance for solar energy applications and solar radiation models," *Sol. Energy* **76**(4), 423–453 (2004).
22. R. L. Kurucz, "Synthetic infrared spectra," in *Infrared Solar Physics*, *IAU Symp. 154*, D. M. Rabin and J. T. Jefferies, Eds., Kluwer Academic, Norwell, MA (1992). (Data available at: http://rtweb.aer.com/solar-frame.html.)
23. P. Kiedron, J. Schlemmer, J. Slusser, and P. Disterhoft, "Validation of ozone and aerosol retrieval methods with UV rotating shadowband spectroradiometer (RSS)," *Proc. SPIE* **6362** (2006).
24. L. Harrison and J. Michalsky, "Objective algorithms for the retrieval of optical depths from ground-based measurements," *Appl. Opt.* **33**, 5126–5132 (1994).
25. C. D. Goering, T. S. L'Ecuyer, G. L. Stephens, J. R. Slusser, G. Scott, J. Davis, J. C. Barnard, and S. Madronich, "Simultaneous retrievals of column ozone and aerosol optical properties from direct and diffuse solar irradiance measurements," *J. Geophys. Res.* **110**, D05204 (2005).

Biographies and photographs of the authors not available.